nanoPaint: dynamic imaging of nanoscopic structural plasticity of the plasma membrane

Mariana Tasso[*], *Thomas Pons, Nicolas Lequeux, Julie Nguyen, Zsolt Lenkei* and *Diana Zala*[*]

Dr. M. Tasso
The Research Institute of Theoretical and Applied Physical Chemistry (INIFTA), CONICET, National University of La Plata, Diagonal 113 y calle 64, B1906ZAA La Plata, Argentina.
E-mail: mtasso@inifta.unlp.edu.ar

Dr. T. Pons, Prof. N. Lequeux
LPEM, ESPCI ParisTech, PSL Research University, CNRS UMR 8213, Sorbonne Universités, 10 rue Vauquelin, 75005 Paris, France.

Julie Nguyen, Dr. Z. Lenkei, Dr. D. Zala
Brain Plasticity Unit, ESPCI ParisTech, PSL Research University, CNRS UMR 8249, Paris, France. Center of Neuroscience and Psychiatry, INSERM U894, Paris Descartes University, 102-108 rue de la Santé, 75015 Paris, France.
E-mail: diana.zala@inserm.fr

Keywords: super-resolution microscopy, quantum dots, cannabinoid receptor type 1, neuronal plasticity, synapses

Abstract

Single-particle tracking with quantum dots (QDs) constitutes a powerful tool to track the nanoscopic dynamics of individual cell membrane components unveiling their membrane diffusion characteristics. Here we tested the possibility of extracting from the nano-resolved (16 ms and 30 nm) population dynamics of several quantum dots, time-binned at the second time-scale, the rapid structural changes of the cell membrane surface. We used for this proof-of-concept study bright, small and stable biofunctional QD nanoconstructs recognizing the neuronal cannabinoid type 1 (CB1) receptor and a commercial point-localization microscope to reconstruct in 3D the dynamics of the plasma membrane surface of cultured cells with a spatial resolution of tens of nanometers. CB1 receptor was chosen because it's a highly expressed and fast diffusing membrane protein. Therefore, rapid QD diffusion on the axonal plasma membrane of cultured hippocampal neurons allowed highly precise reconstruction of the membrane surface in less than one minute. QD nanoconstructs diffused into the membrane of synaptic clefts allowing the entire topological reconstruction of the presynaptic component. In addition, we demonstrated successful reconstruction of the remarkably high dynamics of membrane surface topology at the second time-scale both in HEK-293 cell filopodia and axons. Our results show that this novel technique, which we named nanoPaint, is a powerful precision tool for the study of the structural plasticity of cell membrane surfaces.

Introduction

The surface topology of most cell types is continuously adapting to intracellular and extracellular cues. In neurons, rapid structural modifications of the synapse, the relay of neuronal information, is one of the fundamental processes of learning and memory. This was shown in dendritic spines, the typical post-synaptic component in excitatory synapses, with tightly linked structure and function (Segal, 2017). However, it is still unknown if the presynaptic bouton adapts its shape during functional plasticity. Indeed, observation of the presynaptic bouton is typically below the optical resolution limit required for visualization methods relying on Super-Resolution Microscopy (SRM). The major bottleneck of SRM techniques for dynamic studies is the time required to obtained enough information to reconstruct membrane shapes with enough accuracy, which requires usually tens of minutes time-scale, thus precluding the use of this technique to more rapid events.

Single Molecule Localization Microscopy (SMLM) belongs to the recently-developed SRM modalities for fluorescent probes whose spatial and temporal resolution gives now access to domains and events of high biological relevance (Lambert and Waters, 2016; Jin et al., 2018). At large, SMLM has been applied to the translation of fluorescence emission intensities into spatial coordinates, thereby enabling single-particle tracking with unprecedented detail (Shen et al., 2017). In cell biology, SMLM has found plentiful applications in tracking the dynamics of cell membrane components (Dahan et al., 2003; Lidke et al., 2004; Jin et al., 2010; Kovtun et al., 2015), intracellular structures (Andrews et al., 2008; Lowe et al., 2010; Izeddin et al., 2011; Wang et al., 2014; Jungmann et al., 2016), endocytic pathways (Liu et al., 2011; Bhatia et al., 2016) among others.

In particular, Point Accumulation for Imaging in Nanoscale Topography (PAINT) modalities have emerged as a powerful and versatile techniques for reconstruction of super-resolved images of biomolecular structures and cell membranes (Sharonov and Hochstrasser, 2006; Giannone et al., 2010; Jungmann et al., 2014; Aloi et al., 2016). This technique relies on the super-localization of individual fluorophores bound to the target of interest. The photobleached probes are continuously replaced by a large pool of free, unbound fluorophores present in the solution. However, the dynamics of exchange between photobleached and new unbleached fluorescent probes is slow. This process can be accelerated by increasing the concentration of free probes in solution, though this increases the fluorescent background and eventually prohibits the detection of isolated bound fluorophores. In practice, fully reconstructed images often require acquisition durations of several tens of minutes, thereby preventing the study of fast dynamic events. This limitation may be lifted using FRET–based

probes (Auer et al., 2017), though at the expense of adding two fluorophores, complex antibody-DNA constructs and finely-tuned complementary strands. Noteworthy, this technique has so far only been demonstrated for fixed cells (Legant et al., 2016; Lee et al., 2017; Deußner-Helfmann et al., 2018).

The use of quantum dot (QD) nanoparticles as alternative fluorescent probes in highly sensitive biological imaging has witnessed major advances, with the QDs becoming instrumental in several SRM techniques due to their intrinsic brightness, enhanced photostability, broad excitation, narrow and tunable emission wavelengths (Michalet et al., 2005; Pons and Mattoussi, 2009; Mattoussi et al., 2012; Yang et al., 2016; Jin et al., 2018). By combining SRM with brilliant and robust fluorescent probes as the QDs, it is possible to follow the rapid dynamics of cell membrane components, like receptors or transporters, with high temporal and spatial resolution. Cumulative integration of the localization of rapid co-diffusing ligand-target pairs in the 3D-fluid cell membrane can potentially enable the reconstruction of the plasma membrane morphology and follow its changes in nanoscopic cellular volumes. Such approach was recently used to create a diffusion and morphological map of the axonal initial segment (Albrecht et al., 2016) and of dendritic spines (Izeddin et al., 2011). However, these studies relied on probes that require the genetic expression of a GFP tag on the target molecule followed by the addition of either QDs-streptavidin-anti-GFP(biotin) nanoconstructs (Albrecht et al., 2016) or a primary plus secondary biotinylated antibodies and then QD-streptavidin (Izeddin et al., 2011). To our knowledge, the application of these methods to track an endogenous receptor allowing the reconstruction of the cell membrane in 3D, has not been demonstrated yet.

In this work, our previously-developed biofunctional QD nanoconstructs (Tasso et al., 2015) targeting the type-1 cannabinoid (CB1) receptor, which is a rapidly diffusing cell membrane protein (Mikasova et al., 2008), were used as 'painting' agents in SRM to rapidly reconstitute the cell membrane in 3D with nanoscopic resolution. This method, we named it "nanoPaint", is amenable to track the dynamics of endogenous cellular membrane biomolecules that can be labeled live using antibodies and has proved instrumental to map the topography and morphological changes of cell membranes. Theoretical models associated to nanoPaint experiments indicate that the extent of the topographic reconstruction of the cell membranes after a given time depends upon the surface density of the nanoconstructs, which is easily controlled by tuning the concentration of the nanoprobes in the cell medium. Because the access of the nanoconstructs into the synaptic cleft is possible, nanoPaint made it possible to rapidly draw (in less than 1 minute) a nanoscopic 3D map of the pre-synapses. Insights of spontaneous,

nanometric membrane deformation in HEK-293 cells and in neurons add versatility to the nanoPaint method and highlight its potential as a precision tool for neuronal plasticity studies.

Main text

The red-emitting (λ_{em} = 650 nm) CdSe/CdS/ZnS multishell quantum dots employed in this work were synthesized following published protocols (Yu and Peng, 2002; Li et al., 2003). These inorganic nanoparticles are capped with vinylimidazole-sulfobetaine copolymer ligand that bears primary amine side chains to be used for bioconjugation (Tasso et al., 2015). These QD nanoparticles demonstrated: a) high colloidal stability and a conserved photoluminescence in the pH range 7–12, b) minimal non-specific interactions with cells in culture and c) a remarkable colloidal stability in the cell cytoplasm after electroporation and follow-up for ~50 h (Tasso et al., 2015). Such properties are essential for proposing these nanoprobes as tools for biological/cellular investigations as they ensure minimal non-specific interactions with the cell membrane and with non-targeted species. In addition, the QDs were rendered bio-specific by oriented immobilization of whole antibodies via an intermediate protein A layer (Tasso et al., 2015). Once the protein A layer was bound to the nanoparticles, the resulting QDs-pA nanoconstructs were kept at pH 7.5 buffer and used as needed for binding to selected antibodies (Ab) simply by mixing a 1:4 QD:Ab ratio. The QD-pA nanoconstructs (**Figure 1**a) thus constitute a universal platform for the oriented immobilization of whole antibodies, thereby providing high versatility to the nanoPaint approach since Abs can be raised against most transmembrane proteins, cell receptors or other membrane-confined biomolecules.

For the proof-of-concept demonstration of nanoPaint method we used the CB1 receptor as the membrane target. The CB1 receptor, one of the most abundant G protein-coupled receptors in the brain, is the target of marijuana and endocannabinoid ligands and well recognized for its capacity to modulate synaptic plasticity and neuronal development (Castillo et al., 2012; Gaffuri et al., 2012). The CB1 receptor has been shown to constitutively cycle between cell membrane and cytoplasm via the endocytic pathway (Leterrier et al., 2004). In neurons, this cycling is necessary for the axonal targeting of the receptor, which is first expressed in the somato-dendritic compartment, endocytosed and actively transported into the axonal compartment where it resides on the cell membrane (Simon et al., 2013). The CB1 receptor has a highly polarized distribution and is mainly found in axons, thus it is a good membrane marker of the axonal and pre-synaptic compartments. Both single molecule tracking and Fluorescence Recovery after Photobleaching (FRAP) methods have indicated high membrane diffusion rates for the CB1 receptor making it a useful reporter for PAINT approaches (Mikasova et al., 2008;

Simon et al., 2013). We evaluated the endogenous CB1 receptor and as an overexpressed FLAG-CB1-GFP (Green Fluorescent Protein, GFP) fusion protein (Leterrier et al., 2004, 2006) (**Figure 1**b). Heterologous intracellular expression of the CB1 receptor fluorescent GFP tag allows easy recognition of receptor-expressing neurons and a control to evaluate the specificity of recognition of the CB1 receptor by the biofunctional QDs. The FLAG-CB1-GFP and endogenous CB1 receptors were detected with, anti-FLAG and anti-CB1 monoclonal Abs, respectively (**Figure 1**b). The QD-Ab bioconjugates resulting from binding of the anti-FLAG Abs to QD-pA nanoconstructs had an overall diameter of ~27 nm and possessed 1–2 fully functional Abs per dot (Tasso et al., 2015).

Throughout this work, typical experiments involved exposure of primary cultures of rat hippocampal neurons to diluted suspensions of QD bioconjugates (1–3 nM) followed by microscopic monitoring. One of the first insights of the notorious difference between single-particle tracking observations with QDs compared to GFP-expressing receptors was obtained by tracing kymographs depicting the temporal movement of both QD nanoconstructs bound to CB1 receptors and GFP-tagged receptors (**Figure 1**b and **Figure S1**). Kymographs, which depict the position along neurites and signal intensity variations of an emitter as a function of time highlight distinct patterns (**Figure 1**d): QDs produce trace patterns of receptor movement that are sharp, oscillatory and well contrasted compared to the surrounding areas thanks to QDs' salient brilliance and to the fact that, at short times after the addition of the nanoconstructs, only a subpopulation of the membrane CB1 receptors is bound to the QDs (see Figure 1c and **VideoS1**, QD panel as opposed to the FLAG-CB1-GFP panel). Being able to tune the QD concentration in the cell medium results in a subpopulation of the receptor to be tracked, thus facilitating single-particle analysis. GFP-related kymographs, on the other hand, could only be constructed for GFP clusters present in endosomes since the green GFP signal is widespread on the cell membrane (see **Figure 1**c, FLAG-CB1-GFP panel) and can therefore not be identified as a single-particle object by current analytical tools. Finally, the maximal projection of the 2 minutes long recording (**Figure 1**c) showed that the majority of neurites have been completely covered by the localizations of QDs, suggesting that the PAINT approach using overexpressed CB1 receptors is able to efficiently label the surface of the plasma membrane in less than 2 minutes.

After having demonstrated both the specific recognition of CB1 receptor by the QD bioconjugates (see also our previous work (Tasso et al., 2015)), and the capacity of plasma-membrane labeling, we used super-resolution microscopy for single-particle tracking at high spatio-temporal resolution. Noteworthy, since the QD solution is never removed from the cell

medium, there is a continuous availability of QD nanoconstructs allowing the visualization of receptor population dynamics over sufficiently long periods of time (~hours) without photobleaching. Furthermore, the concentration of QDs in solution can be easily adjusted throughout the experiment in order to modify the surface density of QDs over time. Importantly, the experiments reported here were carried out under highly inclined thin illumination (HILO) (Tokunaga et al., 2008), implying that we can tune the excitation of the QDs to thin sections containing the structure to be reconstructed. In addition, the fast acquisition rate ensures that only receptor-bound QDs displaying a slower diffusion coefficient as compared to the free QDs in the medium, will be recognized as single particles by the detection algorithms (Giannone et al., 2010).

With the nanoPaint approach it is possible to obtain a sequential reconstruction of the cell membrane by superimposing the localization of several QDs (**Figure 2**). Increasing the acquisition time (*i.e.* increasing the number of frames whose spatial coordinates are superimposed) increases surface coverage, allowing to reconstitute the shape and location of entire filopodes or synaptic buttons, as demonstrated below. This wealth of information is independent on the *ad-hoc* optimization of fluorescent probes (such as those required for PALM microscopy), the reliance on cell fixation or on laborious techniques like TEM, both prone to introduce artifacts (Giepmans et al., 2005; Schnell et al., 2012), or the need for pre-incubation steps with antibodies prior to QDs' introduction (Izeddin et al., 2011). These very bright fluorescent nanoconstructs permit a lateral resolution below 45 nm as measured by Fourier ring correlation (Nieuwenhuizen et al., 2013) and an axial resolution of 85 nm as measured by fiduciary markers (QDs unspecifically bound to the coverslip). The nanoPaint method may thus be performed both for single-particle tracking and for membrane surface reconstruction.

The efficacy of cell surface reconstruction depends both on the number of QDs whose trajectories are being followed and on the acquisition frequency (number of frames per second). In our experience, in particular for transfected cells, coverage also depends on the transfection rate and the specific cellular sub-compartment imaged (soma, dendrites or axons). As observed in **Figure 2**, some areas on the full field of view may appear less well reconstructed than others depending on whether the cell membrane itself and/or the QD nanoconstructs that are possibly "painting" that area are close to the focal plane or not. In general, assuming a random, uncorrelated motion of QDs, the reconstructed area fraction f is given by Equation 1, where d is the QD surface density and A_1 is the area reconstructed by one QD.

$$f = 1 - e^{-dA_1} \qquad (1)$$

Assuming a 2D Brownian motion of the QDs on the cell surface, simulations show that the reconstructed area A_1 depends on the diffusion coefficient D and on the time (**Figure S2**a,b). For slowly diffusing QDs, A_1 initially increases with D, then saturates when the mean-square displacement between two consecutive images becomes larger than the resolution of the reconstructed trajectory (Figure S2c). After reconstructing diffusion trajectories of single anti-FLAG QDs targeting FLAG-CB1-GFP transmembrane receptors, we obtained an average diffusion coefficient $D \approx 0.19$ $\mu m^2 s^{-1}$ (165,000 reconstructed displacements). This is consistent with a previous estimation of 0.175 $\mu m^2 s^{-1}$ obtained by single-particle tracking in cultured neurons (Mikasova et al., 2008). With this diffusion coefficient, simulations predict that the covered membrane area fraction should follow an exponential law with time (**Figure S2**c; Equation 2). The characteristic reconstruction time τ depends on the QD density, d, with $\tau \sim 58\ d^{-1}$ ($s \cdot \mu m^2$) assuming a 20 nm reconstruction resolution and a 16 ms time lag between two consecutive acquisitions.

$$f(t) \sim 1 - e^{-t/\tau} \qquad (2)$$

In both ROIs presented as examples in Figure 2, the QD density was approximately 0.2 μm^{-2}. These membranes should then be theoretically covered (i.e. reconstructed) at 50% in about 185 s (Figure S2d). As shown in Figure 2, this theoretical estimation is consistent with experimental observations. While these simulations enable the estimation of the average reconstruction time for a given target density, the final membrane reconstruction speed relies on random QD blinking and on stochastic Brownian motion in each specific ROI. We can predict that, at this reconstruction resolution, faster diffusion coefficients would not strongly improve the reconstruction speed (Figure S2b). However, increasing the QD density strongly does (Equation 1; **Figure 2**c,d) and, assuming that target density is not a limiting factor, this is easily implemented by increasing QD concentration in the cell medium. As an example, with a diffusion coefficient of 0.19 $\mu m^2 s^{-1}$ and a QD density of 1 μm^{-2}, on average 50% of the membrane should be reconstructed in 39 s, and 80% in 90s (always assuming a 20 nm reconstruction resolution and 16 ms time lag between two consecutive acquisitions).

After calibration of the reconstruction parameters, we have investigated whether QDs-anti-FLAG bound to overexpressed FLAG-CB1 receptors are able to access and explore the synaptic cleft area (**Figure 3**). The localization of the synaptic region was confirmed by the

expression of tdTomato-Bassoon. Bassoon is a large multi-domain protein of the presynaptic active zone used here to identified the presynaptic component (tom Dieck et al., 1998; Gundelfinger et al., 2016). Super-resolution point accumulation of QD trajectories around the areas of high Bassoon expression reveals a high frequency of visit for the QD nanoconstructs accessing the synaptic cleft (note the brighter regions at the active zones) as well as a remarkable reconstruction of the contours of presynaptic buttons (**Figure 3a**). With addition of cylindrical lens and localization of QDs it is possible to generate a 3D image of the synaptic buttons and the synaptic cleft within a 5 min acquisition that matches other representations of the same areas obtained by more laborious techniques, such as transmission electron microscopy (Burette et al., 2015) (**Figure 3**b and **VideoS2**). Since surface reconstruction of a given cell membrane region is dependent of the effective 'exploration' by the biofunctional QDs during live cell imaging, it is noteworthy that our ~27 nm in diameter QD nanoconstructs appropriately accessed and explored the synaptic cleft. In a pioneering work, Dahan *et al.* demonstrated that slightly larger QD bioconjugates (QD-streptavidin bound to a secondary plus primary antibody) could be detected in the synaptic cleft, where they possessed smaller coefficients of diffusion as compared to the extra-synaptic QDs (Dahan et al., 2003). On the other hand, a recent study comparing different sizes of nanoconstructs recognizing the post-synaptic AMPA receptor, which has an extracellular domain of 12 nm, showed that steric impairment hampers the accessibility and diffusion into the synaptic cleft for large QD-streptavidin nanoconstructs (>20 nm in diameter) (Lee et al., 2017). Recognizing the relatively small extracellular domain of CB1 receptor, our QDs appear to be small enough to access and effectively map the entire topography of presynaptic boutons in mature synapses.

Having gained insight into surface coverage abilities of nanoPaint, we investigated the capability to explore structural plasticity at a nanoscale level with a time resolution below 1 minute, a relevant time scale for cytoskeletal changes. At first, we tested the method in a model cell line (HEK-293 cells) expressing the FLAG-CB1-GFP (Leterrier et al., 2006) receptor and for which we had previously demonstrated the binding specificity of the QDs-pA-anti-FLAG nanoconstructs (Tasso et al., 2015). We recorded filopodia, small organelles known to display a highly dynamic behavior, close to the glass surface, which is illustrated in **Figure 4**a with a 320 s time projection. The higher magnification shows two consecutive reconstructions of 16 s (1000 frames) in green and in magenta of a filopodium, with a cross-section of 200 nm as measured by the distance between the two peaks of intensity of the plasma membrane. Moreover, the y-z cross section indicates that the membrane reconstruction was also efficient in 3D since the reconstruction is covering almost the entire depth of the filopodium; only the

bottom is not visited by the QDs, probably due by their difficulty to access this region which is close to the coverslip. The comparison of the two consecutive 16 s reconstructions revels that the filopodium is elongating and bending at the tip during this time period. To quantify the structural modification, we have measured the distance between both reconstructions by tracing a line scan profile and recorded a 85 nm shift of the tip between the two consecutive 16 s recording time-frames. The nanoPaint method is thus able to measure rapidly and accurately nanoscopic deformations of plasma membrane delimited organelles such as filopodia.

Finally, we evaluated the membrane surface mapping capacity of the nanoPaint method by targeting the endogenous CB1 receptor in cultured hippocampal neurons. We investigated the binding specificity of the QDs-pA-anti-CB1 nanoconstructs to the endogenous CB1 receptor. As observed in **Figure S3**a, the endogenous receptor is highly enriched in axons although it is also ubiquitously present in the plasma membrane of the somato-dendritic compartment, as reported previously (Leterrier et al., 2004). The same can be confirmed for the QDs-pA-anti-CB1 nanoconstructs (Figure S3b), with an overlap coefficient of 0.85 (Bolte and Cordelières, 2006). By employing QDs recognizing the endogenous CB1 receptor, we observed that spontaneous membrane deformations could be recorded in hippocampal neurons with nanometric precision and methodological simplicity (**Figure 4b**). Interestingly, the comparaison of 4 consecutive reconstructions of 80s time frames revealed several topological changes in each time frame. The enlargements on the right show a progressive shift of the plasma membrane (**Figure 4b** 1); the formation of a protrusion that could represent the formation of a new branch (**Figure 4b** 2) and deformations of two protrusions (**Figure 4b** 3) and (**Figure 4b** 4). Altogether, these results show that QD bioconjugates recognizing epitopes present at the extracellular space of the plasma membrane are effective, easy and rapid tools to reconstruct in conjunction with SRM in 3D the topology and dynamics of the cellular plasma membrane at a nanoscopic level with high temporal-spatial resolution and long-term imaging potentiality. Given the capability of the bioconjugates to access and explore the synaptic cleft, a road of opportunities opens up to explore neuronal plasticity with the nanoPaint method.

Acknowledgements

This work was supported by the NanoCTC (ANR-10-Nano-05) grant managed by the French Agence Nationale de la Recherche, PSL Nanopaint (Aux Frontières des Labex). The authors wish to acknowledge Maureen McFadden for help with cell culture. Jérémy Ferrier and Renata Santos for critical reading of this manuscript. MT acknowledges CONICET for funding

destined to research and to international mobility. D. Zala and Z. Lenkei contributed equally to this work.

References

Albrecht D, Winterflood CM, Sadeghi M, Tschager T, Noé F, Ewers H (2016) Nanoscopic compartmentalization of membrane protein motion at the axon initial segment. J Cell Biol 215:37–46.

Aloi A, Vilanova N, Albertazzi L, Voets IK (2016) iPAINT: a general approach tailored to image the topology of interfaces with nanometer resolution. Nanoscale 8:8712–8716.

Andrews NL, Lidke KA, Pfeiffer JR, Burns AR, Wilson BS, Oliver JM, Lidke DS (2008) Actin restricts FcεRI diffusion and facilitates antigen-induced receptor immobilization. Nat Cell Biol 10:955–963.

Auer A, Strauss MT, Schlichthaerle T, Jungmann R (2017) Fast, Background-Free DNA-PAINT Imaging Using FRET-Based Probes. Nano Lett 17:6428–6434.

Bhatia D, Arumugam S, Nasilowski M, Joshi H, Wunder C, Chambon V, Prakash V, Grazon C, Nadal B, Maiti PK, Johannes L, Dubertret B, Krishnan Y (2016) Quantum dot-loaded monofunctionalized DNA icosahedra for single-particle tracking of endocytic pathways. Nat Nanotechnol 11:1112–1119.

Bolte S, Cordelières FP (2006) A guided tour into subcellular colocalization analysis in light microscopy. J Microsc 224:213–232.

Burette A, Collman F, Micheva KD, Smith SJ, Weinberg RJ (2015) Knowing a synapse when you see one. Front Neuroanat 9:100.

Castillo PE, Younts TJ, Chávez AE, Hashimotodani Y (2012) Endocannabinoid signaling and synaptic function. Neuron 76:70–81.

Dahan M, Lévi S, Luccardini C, Rostaing P, Riveau B, Triller A (2003) Diffusion Dynamics of Glycine Receptors Revealed by Single-Quantum Dot Tracking. Science (80-) 302:442–445.

Deußner-Helfmann NS, Auer A, Strauss MT, Malkusch S, Dietz MS, Barth H-D, Jungmann R, Heilemann M (2018) Correlative Single-Molecule FRET and DNA-PAINT Imaging. Nano Lett 18:4626–4630.

Gaffuri AL, Ladarre D, Lenkei Z (2012) Type-1 cannabinoid receptor signaling in neuronal development. Pharmacology 90:19–39.

Giannone G, Hosy E, Levet F, Constals A, Schulze K, Sobolevsky AI, Rosconi MP, Gouaux E, Tampé R, Choquet D, Cognet L (2010) Dynamic superresolution imaging of endogenous proteins on living cells at ultra-high density. Biophys J 99:1303–1310.

Giepmans BNG, Deerinck TJ, Smarr BL, Jones YZ, Ellisman MH (2005) Correlated light and electron microscopic imaging of multiple endogenous proteins using Quantum dots. Nat Methods 2:743–749.

Gundelfinger ED, Reissner C, Garner CC (2016) Role of Bassoon and Piccolo in Assembly and Molecular Organization of the Active Zone. Front Synaptic Neurosci 7:19.

Izeddin I, Specht CG, Lelek M, Darzacq X, Triller A, Zimmer C, Dahan M (2011) Super-Resolution Dynamic Imaging of Dendritic Spines Using a Low-Affinity Photoconvertible Actin Probe Degtyar VE, ed. PLoS One 6:e15611.

Jin D, Xi P, Wang B, Zhang L, Enderlein J, van Oijen AM (2018) Nanoparticles for super-resolution microscopy and single-molecule tracking. Nat Methods:1.

Jin T, Tiwari DK, Tanaka S-I, Inouye Y, Yoshizawa K, Watanabe TM (2010) Antibody-protein A conjugated quantum dots for multiplexed imaging of surface receptors in living cells. Mol Biosyst 6:2325–2331.

Jungmann R, Avendaño MS, Dai M, Woehrstein JB, Agasti SS, Feiger Z, Rodal A, Yin P (2016) Quantitative super-resolution imaging with qPAINT. Nat Methods 13:439–442.

Jungmann R, Avendano MS, Woehrstein JB, Dai M, Shih WM, Yin P (2014) Multiplexed 3D cellular super-resolution imaging with DNA-PAINT and Exchange-PAINT. Nat Meth 11:313–318.

Kovtun O, Sakrikar D, Tomlinson ID, Chang JC, Arzeta-Ferrer X, Blakely RD, Rosenthal SJ (2015) Single-Quantum-Dot Tracking Reveals Altered Membrane Dynamics of an Attention-Deficit/Hyperactivity-Disorder-Derived Dopamine Transporter Coding Variant. ACS Chem Neurosci 6:526–534.

Lambert TJ, Waters JC (2016) Navigating challenges in the application of superresolution microscopy. J Cell Biol:jcb.201610011.

Lee SH, Jin C, Cai E, Ge P, Ishitsuka Y, Teng KW, de Thomaz AA, Nall D, Baday M, Jeyifous O, Demonte D, Dundas CM, Park S, Delgado JY, Green WN, Selvin PR (2017) Super-resolution imaging of synaptic and Extra-synaptic AMPA receptors with different-sized fluorescent probes. Elife 6.

Legant WR, Shao L, Grimm JB, Brown TA, Milkie DE, Avants BB, Lavis LD, Betzig E (2016) High-density three-dimensional localization microscopy across large volumes. Nat Methods 13:359–365.

Leterrier C, Bonnard D, Carrel D, Rossier J, Lenkei Z (2004) Constitutive Endocytic Cycle of the CB1 Cannabinoid Receptor. J Biol Chem 279:36013–36021.

Leterrier C, Laine J, Darmon M, Boudin H, Rossier J, Lenkei Z (2006) Constitutive activation drives compartment-selective endocytosis and axonal targeting of type 1 cannabinoid receptors. J Neurosci 26:3141–3153.

Li JJ, Wang YA, Guo W, Keay JC, Mishima TD, Johnson MB, Peng X (2003) Large-Scale Synthesis of Nearly Monodisperse CdSe/CdS Core/Shell Nanocrystals Using Air-Stable Reagents via Successive Ion Layer Adsorption and Reaction. J Am Chem Soc 125:12567–12575.

Lidke DS, Nagy P, Heintzmann R, Arndt-Jovin DJ, Post JN, Grecco HE, Jares-Erijman EA, Jovin TM (2004) Quantum dot ligands provide new insights into erbB/HER receptor–mediated signal transduction. Nat Biotechnol 22:198–203.

Liu S-L, Zhang Z-L, Sun E-Z, Peng J, Xie M, Tian Z-Q, Lin Y, Pang D-W (2011) Visualizing the endocytic and exocytic processes of wheat germ agglutinin by quantum dot-based single-particle tracking. Biomaterials 32:7616–7624.

Lowe AR, Siegel JJ, Kalab P, Siu M, Weis K, Liphardt JT (2010) Selectivity mechanism of the nuclear pore complex characterized by single cargo tracking. Nature 467:600–603.

Mattoussi H, Palui G, Na H Bin (2012) Luminescent quantum dots as platforms for probing in vitro and in vivo biological processes. Adv Drug Deliv Rev 64:138–166.

Michalet X, Pinaud FF, Bentolila LA, Tsay JM, Doose S, Li JJ, Sundaresan G, Wu AM, Gambhir SS, Weiss S (2005) Quantum Dots for Live Cells, in Vivo Imaging, and Diagnostics. Science (80-) 307:538–544.

Mikasova L, Groc L, Choquet D, Manzoni OJ (2008) Altered surface trafficking of presynaptic cannabinoid type 1 receptor in and out synaptic terminals parallels receptor desensitization. Proc Natl Acad Sci U S A 105:18596–18601.

Nieuwenhuizen RPJ, Lidke KA, Bates M, Puig DL, Grünwald D, Stallinga S, Rieger B (2013) Measuring image resolution in optical nanoscopy. Nat Methods 10:557–562.

Pons T, Mattoussi H (2009) Investigating Biological Processes at the Single Molecule Level Using Luminescent Quantum Dots. Ann Biomed Eng 37:1934–1959.

Schnell U, Dijk F, Sjollema KA, Giepmans BNG (2012) Immunolabeling artifacts and the need for live-cell imaging. Nat Methods 9:152–158.

Segal M (2017) Dendritic spines: Morphological building blocks of memory. Neurobiol Learn

Mem 138:3–9.

Sharonov A, Hochstrasser RM (2006) Wide-field subdiffraction imaging by accumulated binding of diffusing probes. Proc Natl Acad Sci 103:18911 LP-18916.

Shen H, Tauzin LJ, Baiyasi R, Wang W, Moringo N, Shuang B, Landes CF (2017) Single Particle Tracking: From Theory to Biophysical Applications. Chem Rev 117:7331–7376.

Simon AC, Loverdo C, Gaffuri A-L, Urbanski M, Ladarre D, Carrel D, Rivals I, Leterrier C, Benichou O, Dournaud P, Szabo B, Voituriez R, Lenkei Z (2013) Activation-dependent plasticity of polarized GPCR distribution on the neuronal surface. J Mol Cell Biol 5:250–265.

Tasso M, Giovanelli E, Zala D, Bouccara S, Fragola A, Hanafi M, Lenkei Z, Pons T, Lequeux N (2015) Sulfobetaine–Vinylimidazole Block Copolymers: A Robust Quantum Dot Surface Chemistry Expanding Bioimaging's Horizons. ACS Nano 9:11479–11489.

Tokunaga M, Imamoto N, Sakata-Sogawa K (2008) Highly inclined thin illumination enables clear single-molecule imaging in cells. Nat Methods 5:159–161.

tom Dieck S, Sanmartí-Vila L, Langnaese K, Richter K, Kindler S, Soyke A, Wex H, Smalla KH, Kämpf U, Fränzer JT, Stumm M, Garner CC, Gundelfinger ED (1998) Bassoon, a novel zinc-finger CAG/glutamine-repeat protein selectively localized at the active zone of presynaptic nerve terminals. J Cell Biol 142:499–509.

Wang Y, Cai E, Rosenkranz T, Ge P, Teng KW, Lim SJ, Smith AM, Chung HJ, Sachs F, Green WN, Gottlieb P, Selvin PR (2014) Small Quantum Dots Conjugated to Nanobodies as Immunofluorescence Probes for Nanometric Microscopy. Bioconjug Chem 25:2205–2211.

Yang X, Zhanghao K, Wang H, Liu Y, Wang F, Zhang X, Shi K, Gao J, Jin D, Xi P (2016) Versatile Application of Fluorescent Quantum Dot Labels in Super-resolution Fluorescence Microscopy. ACS Photonics 3:1611–1618.

Yu WW, Peng X (2002) Formation of High-Quality CdS and Other II–VI Semiconductor Nanocrystals in Noncoordinating Solvents: Tunable Reactivity of Monomers. Angew Chemie Int Ed 41:2368–2371.

Preprints (www.preprints.org) | NOT PEER-REVIEWED | Posted: 25 October 2018 doi:10.20944/preprints201810.0603.v1

Peer-reviewed version available at Small 2019; doi:10.1002/smll.201902796

Figures

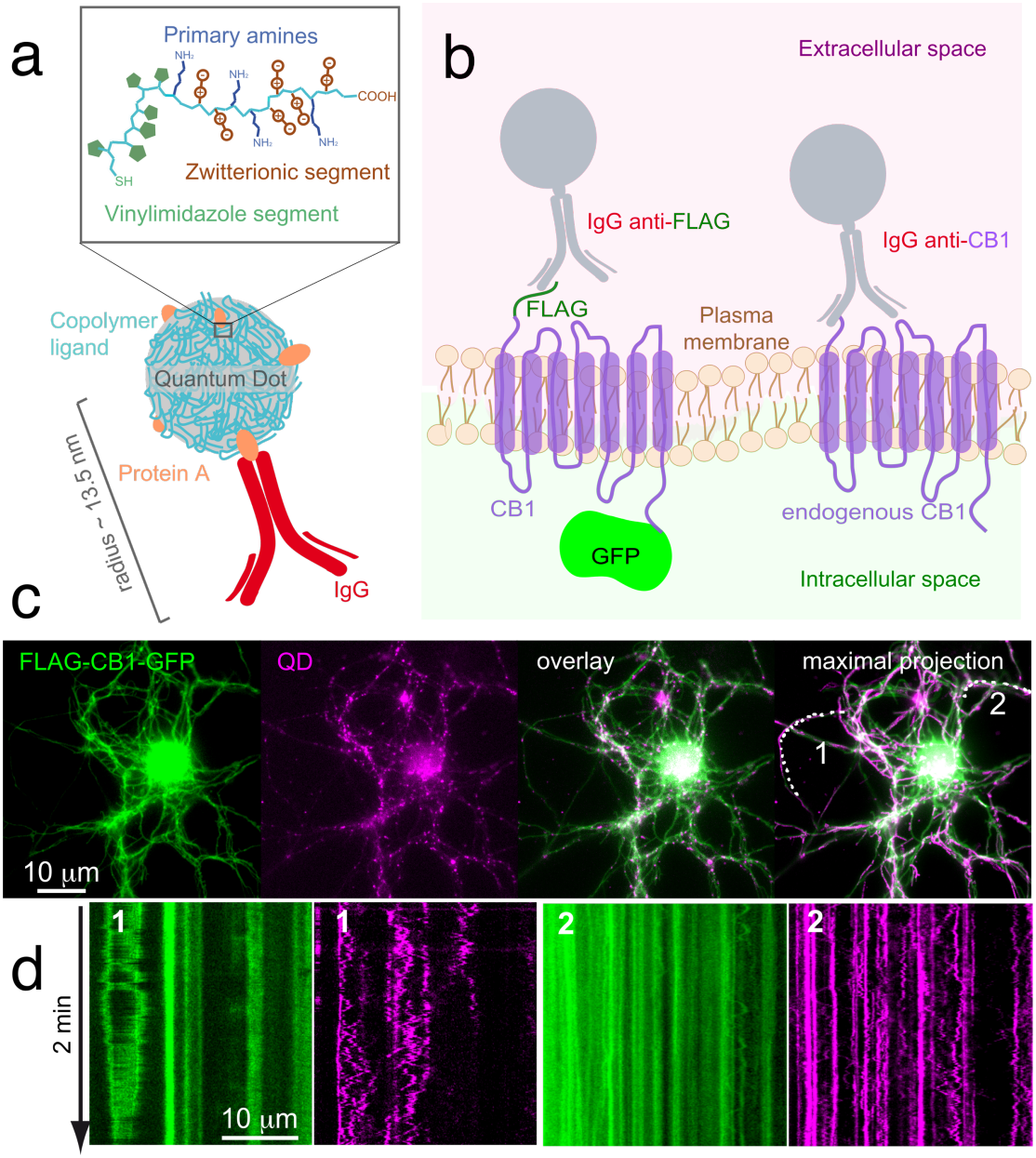

Figure 1. QD-pA nanoconstructs are new nanoprobes for the study of dynamics of membrane proteins. (a) Schematic representation of the biofunctional, fluorescent QD nanoconstructs employed to 'paint' the cell membrane. The nanoconstructs are composed of an inorganic core (quantum dot) surface-covered by vinylimidazole-sulfobetaine copolymer ligand. QDs-pA nanoconstructs result from the reaction of ligand primary amines and protein A, which enable the oriented immobilization of target-recognition IgG antibodies. (b) Illustration of QDs-anti-FLAG used to target the extracellular FLAG tag corresponding to the overexpressed CB1 transmembrane receptor with intracellular GFP terminus (left) and QDs-anti-CB1 employed to

target the endogenous CB1 receptor (right) in live cell experiments. (c) Wide-field epifluorescence images of the FLAG-CB1-GFP and QD channels, their overlay and the maximal projection over a 2-min acquisition time (0.5 fps). Note that, biofunctional QDs allow visualization of the majority of neurites within only 2 min acquisition. (d) Two neuritis from panel c were selected for the kymographs on the GFP (green) and QD (magenta) channels (labeled 1, 2). The Brownian diffusion of QDs is clearly visible on the kymographs, while GFP kymographs are blurrier and appear more static.

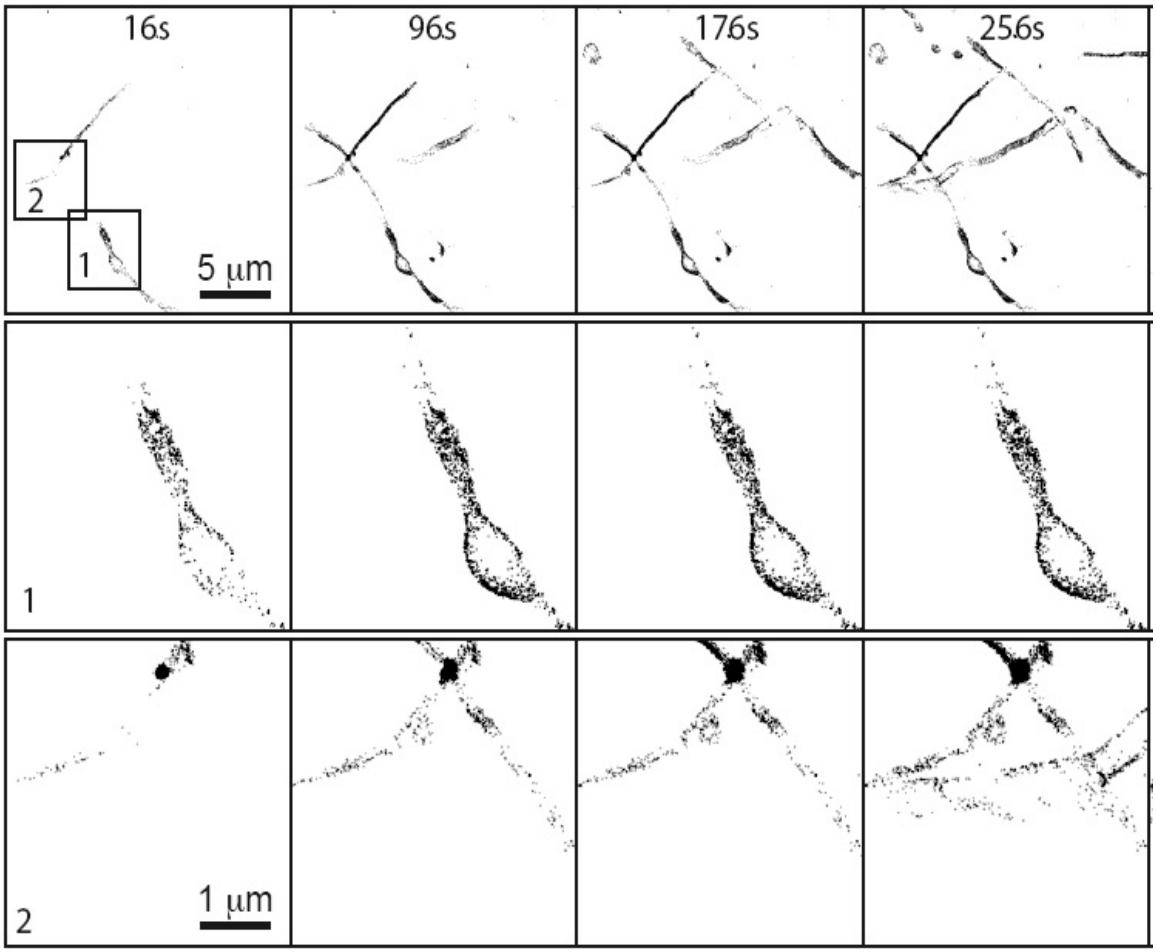

Figure 2 Superimposition of QD localizations over time generates gradual definition of the cell membrane topology. In this example, 21,000 frames (336 s) were sufficient to satisfactorily reconstruct the cell membrane in areas 1 and 2 (rows 1 and 2, respectively). QD-pA-anti-FLAG nanoconjugates labeling FLAG-CB1-GFP expressing neurons: superimposing QD localizations over time produces gradually increasing coverage of the cell membrane topology, with satisfactory levels of membrane reconstruction being achieved by superimposing a certain number of frames. In this example, 21,000 frames (336 s) were sufficient to satisfactorily reconstruct the cell membrane in areas 1 and 2 (rows 1 and 2, respectively).

Preprints (www.preprints.org) | NOT PEER-REVIEWED | Posted: 25 October 2018 doi:10.20944/preprints201810.0603.v1

Peer-reviewed version available at Small 2019; doi:10.1002/smll.201902796

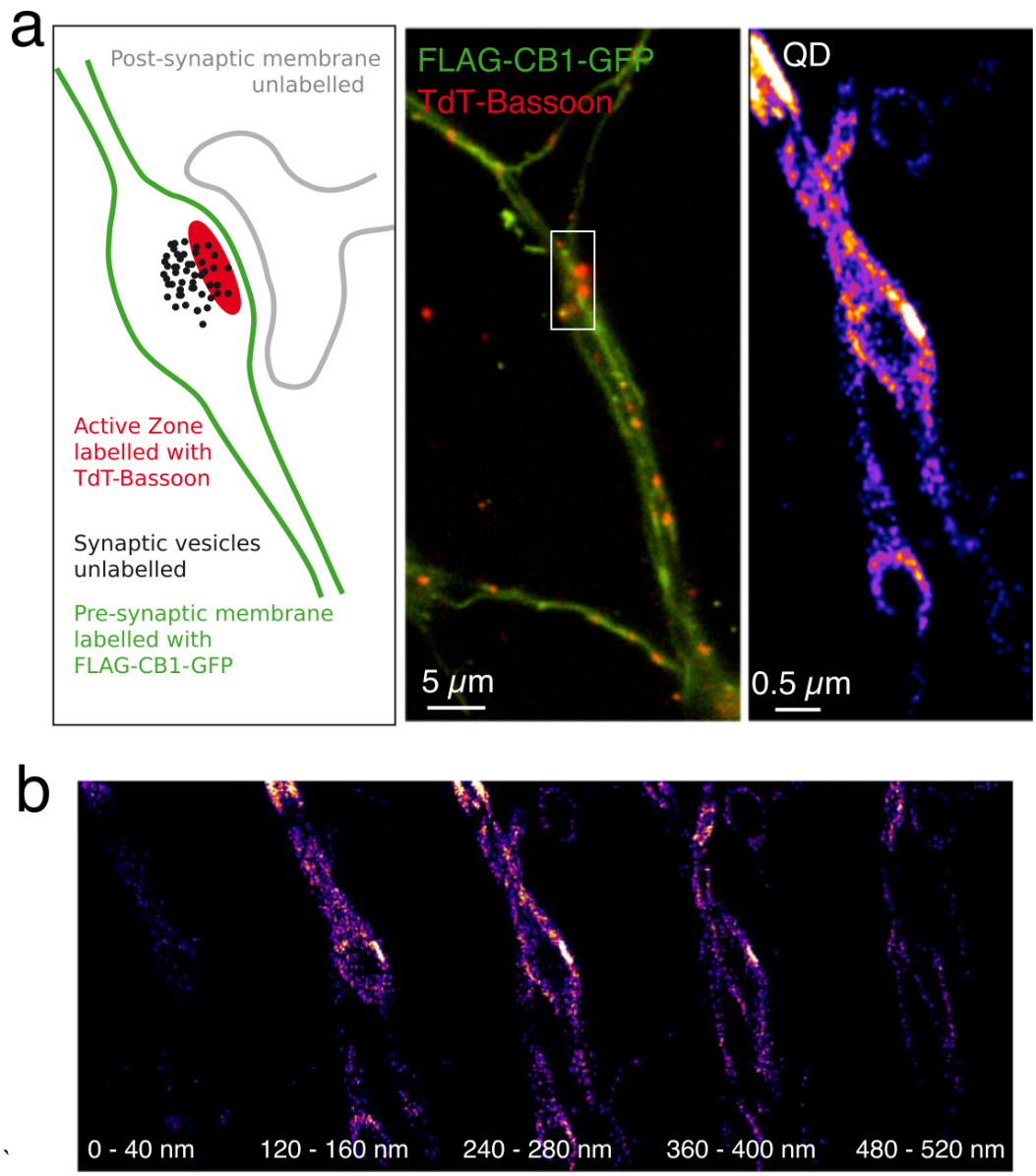

Figure 3. From 2D to 3D cell membrane reconstruction with nanoPaint: Temporal integration of QD localizations around a presynaptic terminal and the use of a cylindrical lens enabled cell membrane reconstruction both in 2D (a, right) and in 3D (b). (a) A schematic representation of the synaptic button and the synaptic cleft is presented (a, left) together with the post and pre-synaptic regions. The localization of the synaptic region is confirmed by the presence of tdTomato-Bassoon (a, middle), a presynaptic marker of the active zone. (b) Membrane reconstruction at different z planes with a depth of 40 nm. For a whole 3D image, see VideoS2. Transfected neurons expressing FLAG-CB1-GFP and tdTomato-Bassoon and QD-pA-anti-FLAG nanoconjugates were used.

Preprints (www.preprints.org) | NOT PEER-REVIEWED | Posted: 25 October 2018 doi:10.20944/preprints201810.0603.v1

Peer-reviewed version available at *Small* **2019**; doi:10.1002/smll.201902796

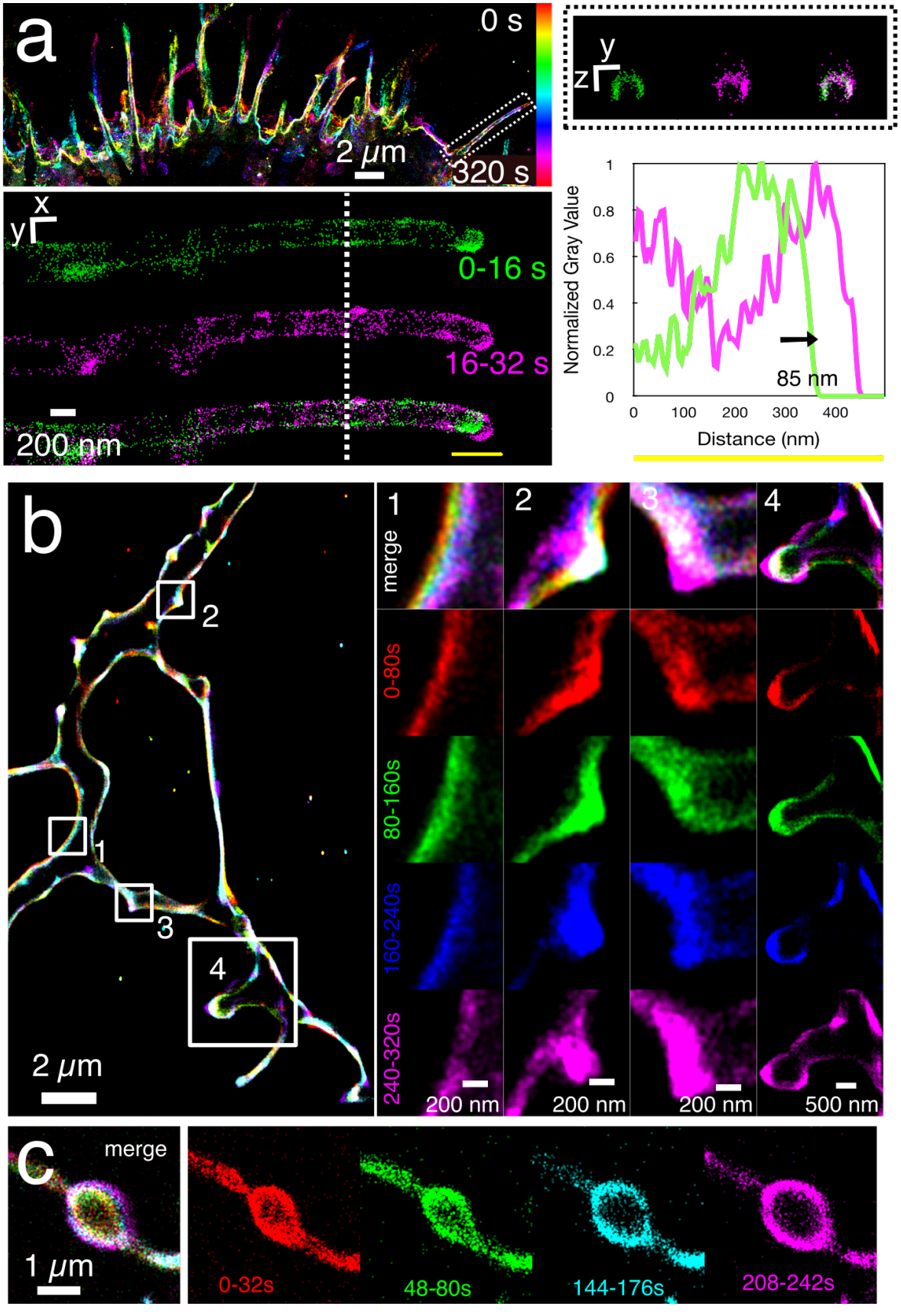

Figure 4. Cell membrane deformation as revealed by nanoPaint. (a) Dynamic reconstruction of the plasma membrane of HEK-293 cells expressing the FLAG-CB1-GFP receptor "nanoPainted" with QDs-pA-anti-FLAG nanoconjugates. On the top left, the color code encodes the temporal reconstruction over 320s. The filopodium on the dashed box is reconstructed in the lower left panel at a higher magnification during the first 16s (green) and the following 16-32s (magenta). The dashed white line represents the plan of orthogonal y-z view showed in the upper right panel. The profile intensity (down right) indicates a shift of the filopodium tip of 85 nm. (b) nanoPaint with QDs-pA-anti-CB1 on DIV50 hippocampal neurons that were reconstructed and color-coded into 5 time-lapses of 80s each. The merged image shows different regions in which spontaneous structural changes have occurred. Four regions were selected for a higher magnification.